Darwinism of Color Image Difference Models

Garrett M. Johnson and Mark D. Fairchild
Munsell Color Science Laboratory, Center for Imaging Science
Rochester Institute of Technology, Rochester New York

Abstract

The world of color image difference modeling can be considered relatively young, when compared with the rich history of general color difference equations. While young, this area of research is well beyond the primordial soup stage. In this paper we present a framework for describing the evolution of color image difference models. This framework builds upon the S-CIELAB model, which in turn was built upon the CIELAB model and the CIE color difference equations.[1] The goal is to create a modular, extendable color image difference model.

Origin of Species

Equations and models for specifying color difference have been a topic of study for many years. This research has culminated in the CIE DE94/2000 color difference equations. These equations have proven to be successful in the prediction of color differences for simple color patches, as well as instrumental based color tolerances. Since they were derived using color patches in well defined viewing conditions, their use in color imaging is less apparent. While these models were never designed for color imaging applications, the successes they enjoy, as well as industry ubiquitousness, serve as a good foundation with which to build upon.

Zhang and Wandell build upon color difference equations nicely with S-CIELAB, a simple extension to CIE-LAB. S-CIELAB adds a preprocessing step to the standard CIELAB equations, which relates to the spatial and color pattern abilities of the human visual system. While this equation has proven to be successful, both with its simplicity and with accuracy, it only represents the first step in the evolution of a more complete Color Image Difference Model.

CSF Growing Pains

S-CIELAB extends upon CIELAB by adding spatial contrast sensitivity filtering as a preprocessing step. The filtering is performed on opponent color channels representing a luminance channel and two chrominance channels, red-green and yellow-blue. The spatial filtering itself is performed using a series of separable one-dimensional convolution kernels. These convolution calculations represent computational and programmatical simplification. It is possible to further extend the S-CIELAB model by replacing the convolution kernels with other, possibly more accurate, contrast sensitivity functions (CSF).

The opponent color space described by Zhang[1] appears to be well suited for the contrast sensitivity modulation, and is shown in Figure 1.
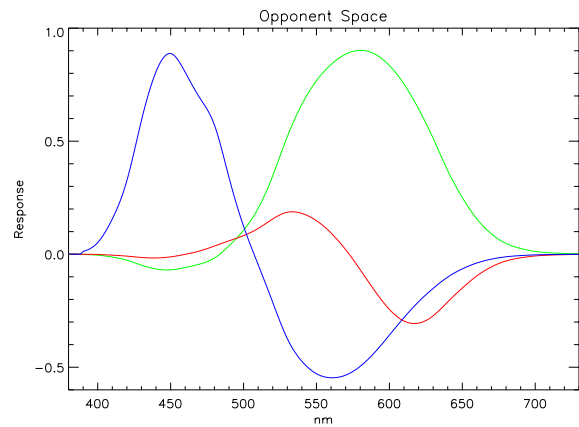

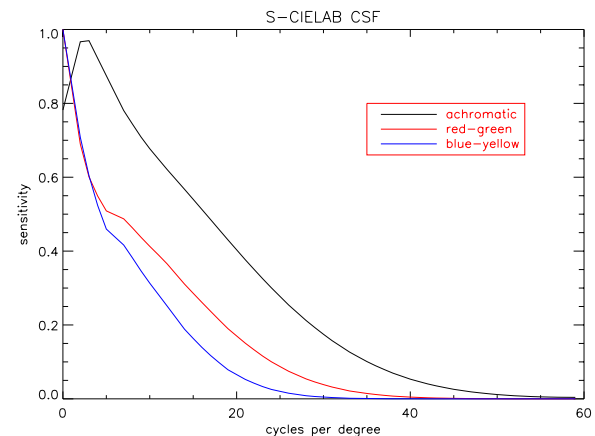*Figure 1. S-CIELAB Opponent Color Space*

Figure 2. Contrast Sensitivity Functions of S-CIELAB

The contrast sensitivity filters used in the S-CIELAB model are based in turn on pattern color separability experiments described by Poirson and Wandell.[2] A series of discrete convolution kernels approximate the filters, as

shown in Figure 2. Fourier theory dictates that the discrete convolution kernels allow only for the sum or difference of cosine waves. These cosine waves are in effect only an approximation of more accurate contrast sensitivity functions. This approximation is balanced out by the ease of implementation and computation of the convolution.

Specifying and implementing the contrast sensitivity filters purely in the frequency, rather than spatial domain, allows for more precise control over the filters. Much research has gone into specifying the luminance contrast sensitivity function.[3,4,5,6] The CSF functions described by Barten[3] and Daly[4] are fully featured models that accurately account for such conditions as luminance level, degree of adaptation, eccentricity, orientation, and many other factors. While all those factors do strongly influence the contrast sensitivity of the human eye, they make for a very complicated model. One of the goals of our model evolution is simplicity, so we have examined a compromise between the very complex CSF models and the convolution model of S-CIELAB. Movshon and Kiorpes describe a three parameter exponential model, as shown in Equation 1, which is a simple description of the general shape of the luminance CSF.[7]

$$csf_{lum}(f) = a \cdot f^c \cdot e^{-b \cdot f} \qquad (1)$$

This equation can be fit to existing luminance contrast sensitivity data sets, when available. Example values for the three parameters are 75, 0.2, 0.8 for a, b, and c respectively, while f is represented in cycles per degree (cpd) of visual angle.[8] This function is then normalized, to produce a filter that modulates between 0.0 and 1.0.

The band-pass nature of the luminance CSF lends itself to certain issues, with respect to its use in imaging applications. Existing color difference equations predict color differences of large uniform areas very well, so it is important that a color image difference metric predict the same results when dealing with uniform patches. In order to do this, it is necessary to maintain the integrity of the DC component (zero cpd). This can be done by converting the band-pass filter to a low pass filter, or by normalizing the CSF so that the DC modulation is set to 1.0. Figure 3 illustrates the differences between these two approaches.

The low-pass CSF function acts to filter out high frequency image differences, similarly to S-CIELAB. The band-pass CSF behaves in a different manner. The relative sensitivities include values that are greater than 1.0, and peak around 4 cycles per degree of visual angle. This serves to enhance any image differences where the human visual system is most sensitive to them. When attempting to predict the perceived visual differences between two images, this enhancement might prove beneficial.

There is considerably less information available regarding the chrominance contrast sensitivity functions. Mullen[9], Van der Horst and Bouman[10], and Poirson and Wandell[2] provide insight into the opponent color contrast sensitivity functions. We have found that the sum of two Gaussian functions, as shown in Equation 2, fit the available data well.

$$csf_{chrom}(f) = a_1 \cdot e^{-b_1 \cdot f^{c_1}} + a_2 \cdot e^{-b_2 \cdot f^{c_2}} \qquad (2)$$

The Van der Horst and Poirson data sets were fit independently and combined, and were shown to have excellent correlation. Table 1 shows the values of the six parameters, for the red-green, and blue-yellow equations that best fit the combined data sets. Figure 4 shows the normalized sensitivities of the two chrominance channels, as a function of cycles per degree of visual angle.
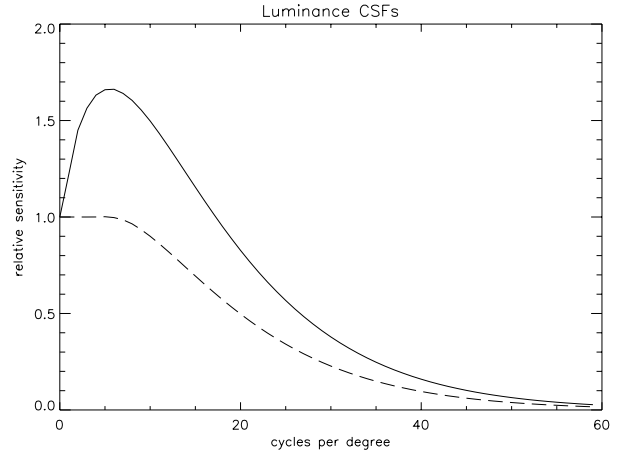

Figure 3. DC Frequency Maintaining CSFs

Table 1. Parameters for Chrominance CSFs

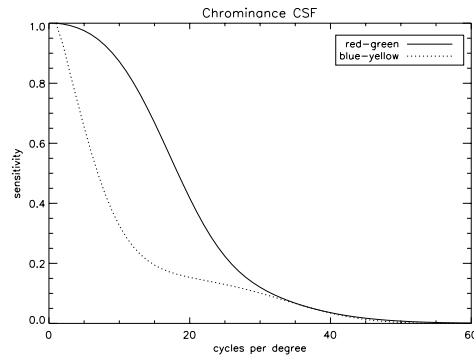| Parameter	Red-Green	Blue-Yellow
a1	109.14130	7.032845
b1	-0.00038	-0.000004
c1	3.42436	4.258205
a2	93.59711	40.690950
b2	-0.00367	-0.103909
c2	2.16771	1.648658

Figure 4. Chrominance CSFs From Eq. 2 and Table 1. The Blue-Yellow CSF is the Dashed Line

Localized Attention

The contrast sensitivity filters as described above generally serve to decrease the perceived differences for high

frequency image information, such as halftone dots. However, it is often observed that the human visual system is especially sensitive to position of edges. The contrast sensitivity functions seem to counter this theory, as edges contain very high frequencies. This contradiction can be resolved if we consider this a type of localization.

The ability to distinguish, or localize, edges and lines beyond the resolution of the cone distribution itself is well documented.[6] While the actual mechanisms of the human visual system might not be known, it is possible to create a simple extension to the existing color image difference models to account for this ability to detect edges.

The simplest such approach is borrowed from the image-processing world. After filtering the opponent channels with the contrast sensitivity functions, a simple edge-enhancing kernel can be applied. We have found that convolution with a common Sobel kernel, such as that shown if Equation 3, works well.

$$x_{dir} = \begin{bmatrix} -1 & 0 & 1 \\ -2 & 0 & 2 \\ -1 & 0 & 1 \end{bmatrix} y_{dir} = \begin{bmatrix} -1 & 2 & -1 \\ 0 & 0 & 0 \\ 1 & 2 & 1 \end{bmatrix} \quad (3)$$

Similar, or perhaps finer tuned filters could be utilized in the frequency domain. This particular Sobel technique does not take into account the cycles-per-degree of the viewing situation, so as a result is not as well tuned for all applications. More research is currently being conducted to produce a more adaptable local attention filter. If this is the case, the filters could even be combined with the above CSFs. Keeping the edge detection separate from the frequency filtering allows for more model freedom, as the actual technique used can be easily swapped with other kernels or filters.

Local and Global Contrast

The ability of an image difference model to predict both local and global perceived contrast differences is very important.[11] This can be considered another area where localization and attention play a factor. Image contrast can often be thought about in terms of image tone reproduction. Moroney[12] presented a local color correction technique based on non-linear masking, which essentially provided a local tone reproduction curve for every pixel in an image. This technique, with its similarity to unsharp masking, can be adapted to provide a method for detection and enhancement of image contrast differences.

This color correction technique generates a family of gamma-correction curves based upon the value of a low-frequency image mask. This can be extended to an image difference model by generating a family of gamma curves for each of the opponent color channels, based not only on the low frequency information at each channel, but also the global contrast of each channel. The low-frequency mask for each image can be generated by filtering each image with a low-pass Gaussian curve. It is often helpful to use a

modified Hanning window to reduce ringing artifacts in the mask. The contrast curves can then be generated using Equation 4. This equation is similar in form to Moroney's technique, while accounting for a positive image mask.

$$gamma = \max \cdot \left[\frac{input}{\max} \right]^{2^{\left\{ \frac{medium}{median - mask} \right\}}} \quad (4)$$

By using the maximum, minimum, and median value of each channel, these gamma curves now become functions of the global image contrast. Care must be taken with the chrominance channels, as they contain both positive and negative values. This can be alleviated by creating families of curves for positive and negative values, or by using absolute values of the input channels. This technique can be easily modified or extended by manipulating the form or parameters of Equation 4.

Orientation and Masking

Orientation selectivity, both in the contrast sensitivity functions as well as in cortical processing can play an important role in the prediction of differences in color images. An evolutionary enhancement to S-CIELAB, and thus our proposed models, has already been formulated with the Color Visual Difference Metric (CVDM).[13] This model uses the Daly modified cortex transform to generate a family of radial and orientation specific spatial frequency reprentations.[4,14] The CVDM uses these representation to create models of visual masking, as well as local contrast. It is easy to extend this model with any of the enhancements described above.

Data Reduction

The output of all of the color image difference models described so far is an error image, where each pixel represents the $CIE\Delta E_{94}$ error between an original and a reproduction. While this image might be very valuable for locating specific problems within an imaging system, often times we would like to reduce the error image to a single error metric. How to perform this reduction is still subject to further research. We have examined many techniques, mostly involving image statistics. One general technique is to simply take the mean color difference of the image. There is no reason to believe that overall perceived difference is a simple averaged weighting. The mean might also mask other valuable information. One common example of this is when comparing images with large variations of individual pixels, such as noise artifacts, with images that have large areas of color difference and similarly large areas with no color differences. The mean error of these two images might be the same, but the large area color difference image will be more perceptibly noticeable. Other image statistics, such as median, image percentiles, skewness, and standard deviation, have also been used with moderate success. In our experience, higher

order image percentiles, standard deviation, and standard deviation normalized by mean-error have proven to have the most success in experimental prediction.

S-CIELAB
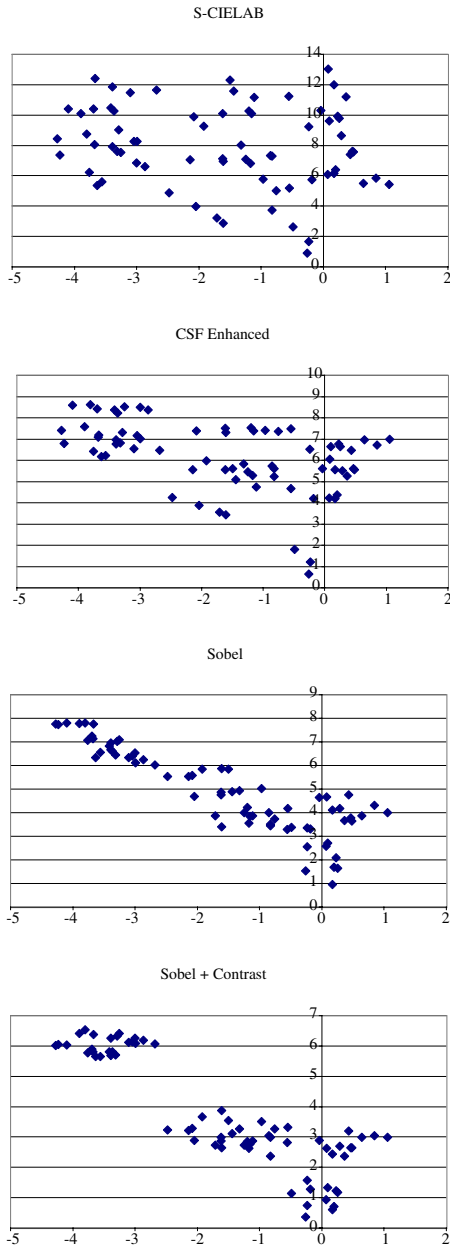
CSF Enhanced

Sobel

Sobel + Contrast

Figure 5. Experimental Verification. The x-axis represents interval difference scale, while the y-axis represents model prediction (standard deviation of error images)

Experimental Verification

We have examined the effects of each of these evolutionary model features on data comparing image sharpness. These data represent an interval scale of perceived sharpness differences between an original image, and 71 varying reproductions. The data reduced output from an ideal color image difference model would have a linear relationship with the interval scale. Figure 5 shows the interval difference scale plotted against the standard deviation of the model outputs. Standard deviation of the error image is thought to correlate well with perception. If two images were to appear to be identical, the resulting error images would have little to no error, and thus a low standard deviation. Likewise, if two images have areas of large error, as well as areas of small error, such as the case for systematic color shifts, the standard deviation will be large. This correlates well with the perception of large systematic errors. Each plot in Figure 5 represents an evolutionary step in complexity. The top plot illustrates the results of S-CIELAB, which serves as base level. The second plot shows S-CIELAB with the modified band-pass enhancing CSF. The third plot adds in the Sobel filter, and the forth adds the contrast detection metric. It can be seen that each modification makes the relationship between the model output and the experimental data become more linear. The forth plot also illustrates the limitations of data reduction to a single number, in this case standard deviation. While more linear, the forth plot also shows a clustering nature, with each cluster representing a certain error artifact. Without more information, it is difficult to separate the clusters into more meaningful representations. This is why care must be taken when reducing error images into single numbers.

Conclusion and Future Work

Using S-CIELAB as a guide, a modular framework for the evolution of color image difference models has been described. The first module began with the simple S-CIELAB contrast sensitivity functions and was extended with more precise filters, as well as a method for enhancing image differences where the human visual system is most sensitive. A simple technique for accounting for localization using edge-enhancing filters was then introduced. Methods for contrast enhancement, orientation, masking, and data reduction were also discussed.

The goal of this framework is to create a viable metric of image fidelity. This metric can be used to test the output of various imaging systems. One such example might be the evaluation of image compression techniques, to determine the perceptual difference caused by the compression. The ultimate goal from this work is to create a foundation for a model of image quality that can predict both image degradations as well as enhancements.

Acknowledgements

References

1. X. M. Zhang and B. A. Wandell, "A spatial extension to CIELAB for digital color image reproduction," *Proceedings of the SID Symposiums* , (1996).
2. B. Poirson and B. A. Wandell, "The appearance of colored patterns: pattern-color separability," *J. Opt. Soc. A.*, (1993).
3. P. G. J. Barten, *Contrast Sensitivity of the Human Eye and Its Effects on Image Quality*, SPIE, Bellingham, WA (1999).
4. S. Daly, The Visible Differences Predictor: An algorithm for the assessment of image fidelity, Ch. 13 in *Digital Images and Human Vision*, A.B. Watson, Ed., MIT Press, Cambridge, (1993).
5. P. Lennie and M. D'Zmura, "Mechanisms of color vision," *CRC Critical Reviews Neurobilogy*, (1988).
6. B. A. Wandell, *Foundations of Vision*, Sinauer Associates Inc. Sunderland, MA (1995).
7. T. Movshon and L. Kiorpes, "Analysis of the development of spatial sensitivity in monkey and human infants," *JOSA A,* vol5 (1988).
8. E. Montag, personal communication, (2000).
9. Mullen, K, "The contrast sensitivity of human color vision to red-green and blue-yellow chromatic gratings," *J. Physiol.*, 359 (1985).
10. G. J. C. Van der Horst and M. A. Bouman, "Spatiotemporal chromaticity discrimination," *JOSA*, 59 (1969).
11. X. Zhang and B. A. Wandell, "Color Image Fidelity Metrics Evaluated Using Image Distortion Maps," *Signal Processing*, 70 (1998).
12. N. Maroney, "Local Color Correction Using Non-Linear Masking," *Proc. of IS&T 8th Color Imaging Conference*, (2000).
13. E.W. Jin, X.-F. Feng, and J. Newell, "The development of a color visual difference model (CVDM)," *IS&T PICS Conference*, 154-158 (1998).
14. B. Watson, "The cortex transform: Rapid computation of simulated neural images," *Computer Vision Graphics and Image Processing*, 39 (1987).
15. G. M. Johnson and M. D. Fairchild, "Sharpness Rules," *Proc. of IS&T 8th Color Imaging Conference*, (2000).

Biography

Garrett M. Johnson is a Color Scientist at the Munsell Color Science Laboratory, as well as a Ph. D. Student in the Center for Imaging Science, at the Rochester Institute of Technology. He has a BS in Imaging Science and a MS in Color Science, both from RIT. His research interests include color image difference and color appearance modelling, image synthesis, and computer graphics. He is a member of ISCC, IS&T, and ACM-SIGGRAPH.